JOURNAL OF SOLID STATE CHEMISTRY **127,** 325–330 (1996)
ARTICLE NO. 0390

The V(III) Monophosphate Series $AV_2O(PO_4)_2$ with A = Cd, Ca, Sr: Structure and Magnetism

S. Boudin, A. Grandin,* Ph. Labbé, J. Provost, and B. Raveau

Laboratoire CRISMAT, ISMRA et Université de Caen, Boulevard du Maréchal Juin, 14050 Caen cedex, France

Received February 7, 1996; in revised form September 19, 1996; accepted September 24, 1996

The strontium vanadophosphate, belonging to the series $AV_2O(PO_4)_2$ with A = Cd, Ca, Sr has been synthesized. Its single-crystal X-Ray study shows its isotypism with the cadmium and calcium phases. It crystallizes in the space group *Pnma* with $a = 14.220(1)$ Å, $b = 6.5138(6)$ Å, and $c = 7.5166(8)$ Å, $Z = 4$, and $R = 0.039$. In its structure, built up from $[V^{III}O_2]_\infty$ rutile chains connected through VO_6 octahedra and PO_4 tetrahedra, the geometry of the polyhedra is very close to that obtained for the Cd and Ca phases. The main difference deals with the V(2)–V(2) intrachains distances that increase significantly with the size of the A cation. The study of the magnetic susceptibility of the three monophosphates (A = Cd, Ca, Sr) evidences a narrow transition of 20 K from a paramagnetic to antiferromagnetic state. This behavior is in contrast with that of the $V^{III}PO_4$ phase that also exhibits isolated rutile chains but shows a broad transition spreading over 100 K. This difference is explained by the presence of additionnal VO_6 octahedra that may weaken the unidimensional character of these phosphates compared to VPO_4.

INTRODUCTION

During the exploration of trivalent vanadium phosphates, two isostructural compounds $CdV_2O(PO_4)_2$ (1) and $CaV_2O(PO_4)_2$ (2) were recently isolated. Their structure is of interest due to the fact that it is built up, like that of VPO_4 (3), from $[VO_2]_\infty$ rutile chains. The latter exhibits indeed unidimensional magnetic properties, due to the isolated character of the rutile chains in the structure. Nevertheless, the cadmium and the calcium vanadium phosphates differ from VPO_4 by the fact that the $[VO_2]_\infty$ chains are linked to additional VO_6 octahedra. For this reason a different magnetic behavior can be expected. Moreover, the V–V distances in the chains that are dictated by the size of the A cation (Cd or Ca) may influence the magnetic properties of these compounds. In order to understand the relationships between the structure and magnetic properties of these phases, we tried to synthesize isotypic compounds with a larger A cation such as strontium. We report herein on the single-crystal structure of the isotypic phase $SrV_2O(PO_4)_2$ and on the magnetic properties of the compounds $AV_2O(PO_4)_2$ for A = Cd, Ca, Sr.

* To whom correspondence should be addressed.

EXPERIMENTAL

Black lamellar single crystals of $SrV_2O(PO_4)_2$ were collected from a mixture of $Sr_3V_4P_6O_{24}$ (nominal composition) and NaCl in a weight ratio 10:1, respectively. The synthesis was performed in two steps. First, $SrCO_3$, V_2O_5, and $H(NH_4)_2PO_4$, in ratio 5:2:10, were mixed and heated at 883 K in order to eliminate CO_2, NH_3, and H_2O. Second, the resulting product was mixed with an appropriate amount of V and NaCl. The mixture $Sr_3V_4P_6O_{24}$. NaCl was placed in an alumina tube and sealed in an evacuated silica ampoule. This sample was heated at 1223 K for 24 hr, slowly cooled at a rate of 1°/hr for 200 hr, and quenched to room temperature. The composition of crystals was confirmed by microprobe analysis.

Polycrystalline $AV_2O(PO_4)_2$ phases (A = Cd, Ca and Sr) were obtained by a two-step method as described in Table 1.

Powder patterns of the $AV_2O(PO_4)_2$ polycrystalline phases (A = Cd, Ca, Sr) were recorded on a Philips diffractometer using the Cu$K\alpha$ radiation. Cell parameter refinement of polycrystalline phases was performed by a least-squares method using the program Fullprof (4).

A black lamellar crystal of $0.051 \times 0.141 \times 0.039$ mm was selected for the structure determination. Cell parameters reported in Table 2 were refined upon 25 reflections with $18° < \theta < 22°$. The data collection was performed on a CAD-4 Enraf–Nonius diffractometer using the Cu$K\alpha$ radiation. Intensities were corrected from the Lorentz and polarization effects. Due to small size and approximative facies of crystal, absorption correction has not been performed. No weighting scheme was applied. The refinement, on the Xtal program (5), of the atomic coordinates and the anisotropic thermal factors, lead to $R = 0.039$ and $R_w = 0.047$.

0022-4596/96 $18.00

TABLE 1
Experimental Conditions for Synthesis of Polycrystalline Phases

Phases	Starting materials	Heating for the first step	Experimental conditions for the second step
$CdV_2O(PO_4)_2$	CdO, 0.6 V_2O_5 $2H(NH_4)_2PO_4$	673 K for 2 hr	In a silica ampoule: (1) at 1473 K for 40 hr (2) slowly cooling at a rate of 2°/hr for 100 hr (3) quenched to room temperature
$CaV_2O(PO_4)_2$	$CaCO_3$, 0.6 V_2O_5 $2H(NH_4)_2PO_4$	1073 K for 24 hr	Under a pressed pellet in a silica ampoule: (1) 1373 K for 24 hr (2) quenched to room temperature
$SrV_2O(PO_4)_2$	$SrCO_3$, 0.6 V_2O_5 $2H(NH_4)_2PO_4$	883 K for 2 hr	In a silica ampoule: (1) 1473 K for 24 hr (2) quenched to room temperature

The magnetic moments of powdered samples were measured from 4.5 to 300 K with a SQUID Magnetometer. The 3000-G field was applied after cooling at 4.5 K. The molar susceptibility χ_M and the inverse $1/\chi_M$ were extracted after correction of the sample holder signal and of the core diamagnetism of the all ions; they are plotted in Figs. 2a–2d.

RESULTS AND DISCUSSION

The atomic parameters of $SrV_2O(PO_4)_2$ obtained from single-crystal study refinements (Table 3) show clearly that this phase is isotypic with the cadmium and the calcium homologous phases. Thus, its structure consists of $[V_2P(1)O_7]\infty$ layers (Fig. 1), connected along **a**, through discontinuous layers of $[P(2)O_4]\infty$. The $[V_2P(1)O_7]\infty$ layers are composed of $[VO_2]_\infty$ rutile chains (labeled V(2)) running along **b**, and interconnected through VO_6 octahedra (labeled V(1)) and PO_4 tetrahedra. Note that the chains built up from the V(1) and V(2) running along **b** are isolated from each other, i.e., do not share the apices of their octahedra.

The interatomic distances (Table 4) show that the geometry of the PO_4 tetrahedra is very similar to that observed in the Cd and Ca phosphates, with P–O distances ranging from 1.50(1) to 1.552(9) Å. In the same way, the V(1) octahedra are not modified by the presence of strontium; one indeed observes V(1)–O distances ranging from 1.897(8) to 2.175(8) Å for the Sr phase, compared to 1.90(1)

TABLE 2
Summary of Crystal Data, Intensity Measurements, and Structure Refinement Parameters for $SrV_2O(PO_4)_2$

1. Crystal data	
Space group cell dimensions	*Pnma* a = 14.220(1) Å α = 90° b = 6.5138(6) Å β = 90° c = 7.5166(8) Å γ = 90°
Volume	696.3(1) Å^3
Z	4
ρ_{calc} (g cm^{-3})	3.77
2. Intensity measurements	
λ (Cu$K\alpha$)	1.5418 Å
Scan mode	$\omega - 2/3\ \theta$
Scan width (°)	1.45 + 0.14 tag θ
Slit aperture (mm)	1.50 + tag θ
Max θ (°)	78
Standard reflections	3 measured every 3000 s
Measured reflections	804
h	$0 \rightarrow 18$
k	$0 \rightarrow 8$
l	$0 \rightarrow 9$
Reflections with $I > 3\ \sigma$	633
μ (mm^{-1})	36.8
3. Structure solution and refinement	
Parameters refined	80
Agreement factors	R = 0.039 R_w = 0.047
Weighting scheme	None
Δ/σ max	<0.004
ρ_{max} (e/Å^3)	1.4
ρ_{min} (e/Å^3)	−1.6

TABLE 3
$SrV_2O(PO_4)_2$: Positional Parameters and Their Estimated Standard Deviations

Atom	x	y	z	B_{eq} (Å^2)
Sr	0.21944(8)	1/4	0.1229(2)	1.46(2)
V(1)	0.3821(1)	3/4	0.1532(3)	0.86(5)
V(2)	0.	1/2	0.	0.90(4)
P(1)	0.1892(2)	3/4	0.1119(4)	0.97(6)
P(2)	0.4389(2)	1/4	0.1450(4)	0.85(6)
O(1)	0.3744(4)	0.437(1)	0.1372(8)	1.3(1)
O(2)	0.2648(6)	3/4	−0.032(1)	1.3(2)
O(3)	0.4864(6)	3/4	−0.005(1)	1.7(2)
O(4)	0.2496(6)	3/4	0.281(1)	1.3(2)
O(5)	0.4452(5)	3/4	0.376(1)	1.1(2)
O(6)	−0.0111(6)	1/4	0.171(1)	1.3(2)
O(7)	0.1266(4)	0.5607(9)	0.1026(8)	1.2(2)

Note. Anisotropically refined atoms are given in the form of the isotropic equivalent displacement parameter defined as $B_{eq} = 4/3\ [\beta_{11}a^{*2} + \beta_{22}b^{*2} + \beta_{33}c^{*2} + \beta_{12}a^*b^* \cos\gamma^* + \beta_{13}a^*b^* \cos\beta^* + \beta_{23}b^*c^* \cos\alpha^*]$.

TABLE 4
Distances (Å) and Angles (°) in the Polyhedra of $SrV_2O(PO_4)_2$

V(1)	O(1)	O(1^{iv})	O(2)	O(3)	O(4)	O(5)
O(1)	**2.048(6)**	4.083(9)	2.868(8)	2.800(9)	2.912(9)	2.897(8)
O(1^{iv})	170.9(3)	**2.048(6)**	2.868(8)	2.800(9)	2.912(9)	2.897(8)
O(2)	85.5(2)	85.5(2)	**2.175(8)**	3.16(1)	2.36(1)	4.00(1)
O(3)	90.3(2)	90.3(2)	101.4(4)	**1.90(1)**	3.99(1)	2.92(1)
O(4)	88.8(2)	88.8(2)	66.9(3)	168.3(4)	**2.114(9)**	2.87(1)
O(5)	94.4(2)	94.4(2)	158.1(3)	100.5(4)	91.2(3)	**1.897(8)**

V(2)	O(5^{v})	O(5^{iii})	O(6)	O(6^{vi})	O(7^{vi})	O(7)
O(5^{v})	**2.033(5)**	4.067(7)	3.335(3)	2.41(1)	2.837(8)	2.865(9)
O(5^{iii})	180.0	**2.033(5)**	2.41(1)	3.335(3)	2.865(9)	2.837(8)
O(6)	108.2(3)	71.8(3)	**2.082(5)**	4.165(7)	2.91(1)	2.863(9)
O(6^{vi})	71.8(3)	108.2(3)	180.0	**2.082(5)**	2.863(9)	2.91(1)
O(7^{vi})	89.4(3)	90.6(3)	90.9(3)	89.1(3)	**1.998(6)**	3.997(8)
O(7)	90.6(3)	89.4(3)	89.1(3)	90.9(3)	180.0	**1.998(6)**

P(1)	O(2)	O(4)	O(7)	O(7^{iv})
O(2)	**1.526(9)**	2.36(1)	2.532(9)	2.532(9)
O(4)	101.2(5)	**1.532(9)**	2.525(9)	2.525(9)
O(7)	112.3(3)	111.5(3)	**1.532(6)**	2.466(9)
O(7^{iv})	112.3(3)	111.5(3)	108.2(3)	**1.523(6)**

P(2)	O(1)	(O1^{i})	O(3^{vii})	O(6^{viii})
O(1)	**1.524(6)**	2.431(9)	2.53(1)	2.49(1)
O(1^{i})	105.8(4)	**1.524(6)**	2.53(1)	2.49(1)
O(3^{vii})	113.6(3)	113.6(3)	**1.50(1)**	2.46(1)
O(6^{viii})	108.1(3)	108.1(3)	107.5(5)	**1.552(9)**

Surrounding of the strontium atom

Sr–O(7)	2.421(6) Å
Sr–O(7^{i})	2.421(6)
Sr–O(1)	2.519(6)
Sr–O(1^{i})	2.519(6)
Sr–O(2^{ii})	2.601(9)
Sr–O(4^{iii})	2.610(9)
Sr–O(5^{iii})	2.989(8)

Symmetry codes

i	x	$-y + \frac{1}{2}$	z
ii	$\frac{1}{2} - x$	$y - \frac{1}{2}$	$\frac{1}{2} + z$
iii	$\frac{1}{2} - x$	$y - \frac{1}{2}$	$z - \frac{1}{2}$
iv	x	$-y + \frac{3}{2}$	z
v	$x - \frac{1}{2}$	$-y + \frac{3}{2}$	$-z + \frac{1}{2}$
vi	$-x$	$-y + 1$	$-z$
vii	$-x + 1$	$-y + 1$	$-z$
viii	$\frac{1}{2} + x$	$-y + \frac{1}{2}$	$-z + \frac{1}{2}$

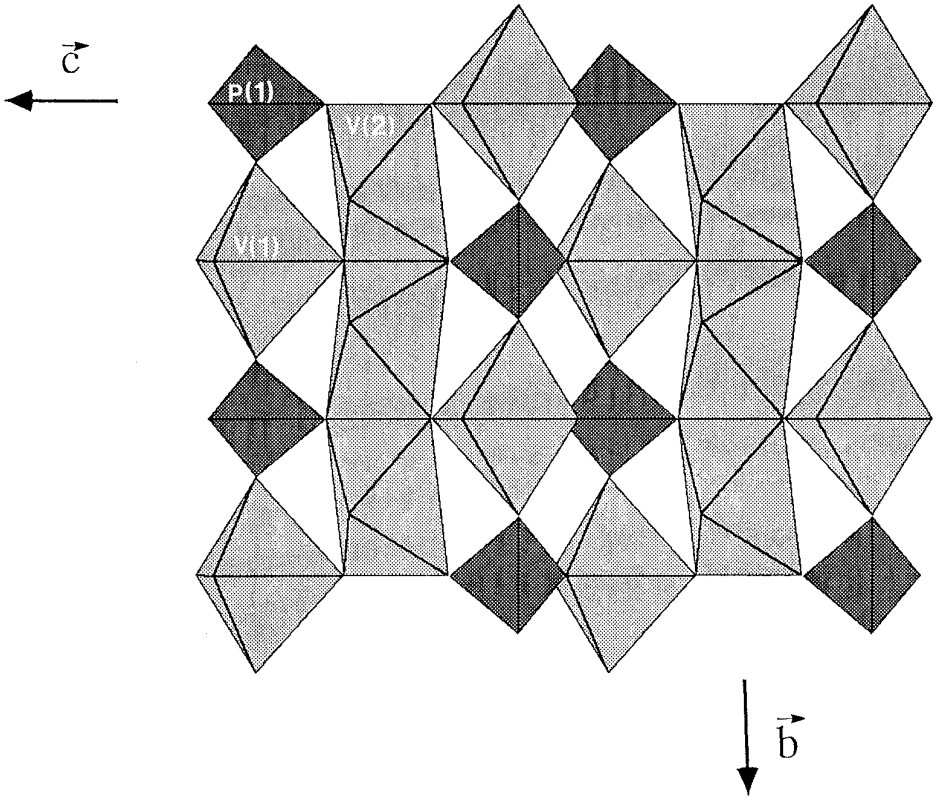

FIG. 1. Projection of the $[V_2P(1)O_7]_\infty$ layers along **a**.

to 2.17(2) Å and 1.897(4) to 2.164(4) Å for the cadmium and calcium phases, respectively. The V(2)–O distances in the Sr phase, ranging from 1.998(6) to 2.082(5) Å, are only slightly larger than those observed for cadmium (1.98(1) to 2.07(1) Å) and for calcium (2.008(2) to 2.071(3) Å).

The Sr^{2+} cation, located at the intersection of the tunnels running along the ⟨011⟩ directions, adopts a "6 + 1" coordination, like Ca^{2+}. The six nearest neighbors are located at distances ranging from 2.421(6) to 2.610(9) Å, instead of 2.28(1) to 2.46(1) Å for cadmium, and of 2.342(3) to 2.519(5) for calcium, in agreement with the relative sizes of these three cations. The seventh Sr–O distance of 2.989(8) Å is close to the corresponding Ca–O distance (2.911(4) Å).

TABLE 5
Distance (Å) V–V in $AV_2O(PO_4)_2$

Phase	V(2)–V(2)	V(1)–V(2)
A = Cd	3.159(1)	3.465(3)
A = Ca	3.212(1)	3.479(1)
A = Sr	3.257(1)	3.501(2)

The main difference between the three structures deals with the V(2)–V(2) distances within the rutile chains (Table 5) that increase significantly from 3.159(1) Å for the Cd to 3.257(1) Å for Sr, and at a lesser degree the V(1)–V(2) distances that range from 3.465(3) to 3.501(2) Å for Sr.

The powder X-ray diffraction of all these phases attest of their great crystalline purity; however, for the Ca phase a green amorphous impurity phase is visually observed by a binocular microscope. These three patterns can be indexed (Table 6) in an orthorhombic cell, with parameters (Table 7) close to those observed from single-crystal studies. Note that b, c, and V increase with the size of the A cation.

The three phases exhibit a transition from an antiferromagnetic state to a paramagnetic at 20 K as T increases (Fig. 2). This transition is characterized by a sharp peak on the $\chi_M(T)$ curves whatever the A cation (Fig. 2a). Above the transition temperature, the $1/\chi_M(T)$ curves (Fig. 2b–Fig. 2d) show that the three compounds follow the Curie–Weiss law, with effective magnetic moments (Table 8), in good agreement with the theoritical value expected for the V(III) ion ($2.83\mu_B$). Note that the calcium phase exhibits a small deviation from the Curie–Weiss law (Fig. 2c), due to the presence of the amorphous magnetic impurity.

TABLE 6
Intereticular Distances and Observed Intensities

$CdV_2O(PO_4)_2$					$CaV_2O(PO_4)_2$					$SrV_2O(PO_4)_2$				
h	k	l	d_{obs} (Å)	I_{obs}	h	k	l	d_{obs} (Å)	I_{obs}	h	k	l	d_{obs} (Å)	I_{obs}
2	0	0	7.151	12.5	2	0	0	7.099	3.6	1	0	1	6.649	11.1
1	0	1	6.462	11.3	1	0	1	6.503	19.2	2	0	1	5.168	8.4
2	0	1	5.089	5.0	2	0	1	5.095	29.4	0	1	1	4.925	1.2
0	1	1	4.759	4.4	0	1	1	4.826	3.8	2	1	0	4.805	3.7
2	1	0	4.732	2.5	1	1	1	4.569	4.7	1	1	1	4.654	1.5
1	1	1	4.515	8.3	2	1	1	3.991	6.4	3	0	1	4.011	2.1
2	1	1	3.962	3.8	3	0	1	3.974	2.2	0	0	2	3.761	9.1
0	0	2	3.622	8.3	0	0	2	3.658	16.7	1	0	2	3.636	100.0
4	0	0	3.575	11.6	1	0	2	3.542	100.0	4	0	0	3.556	5.6
1	0	2	3.511	100.0	3	1	1	3.379	1.6	3	1	1	3.416	5.3
3	1	1	3.368	7.6	2	0	2	3.252	22.5	2	0	2	3.325	5.3
2	0	2	3.231	6.2	0	2	0	3.211	38.6	0	2	0	3.259	37.0
4	0	1	3.206	23.3	4	0	1	3.194	27.4	4	0	1	3.215	20.7
0	2	0	3.156	34.0	4	1	0	3.107	7.6	1	1	2	3.175	1.4
4	1	0	3.111	5.7	1	1	2	3.102	4.5	4	1	0	3.122	6.8
2	2	0	2.887	36.4	2	2	0	2.925	20.8	2	2	0	2.963	17.5
4	1	1	2.858	17.9	3	0	2	2.894	8.3	3	0	2	2.947	1.1
1	2	1	2.836	14.8	1	2	1	2.879	31.8	1	2	1	2.926	18.8
2	2	1	2.682	3.0	4	1	1	2.859	27.7	4	1	1	2.883	22.1
5	0	1	2.660	24.2	2	2	1	2.716	22.3	2	2	1	2.756	5.4
3	1	2	2.623	3.2	5	0	1	2.647	25.8	3	1	2	2.685	9.5
4	0	2	2.545	6.9	4	0	2	2.547	12.4	5	0	1	2.661	23.9
3	2	1	2.473	16.7	3	2	1	2.497	23.5	4	0	2	2.584	16.7
5	1	1	2.452	11.3	5	1	1	2.447	10.6	3	2	1	2.529	16.2
1	0	3	2.381	1.6	0	2	2	2.413	4.4	1	0	3	2.469	2.6
0	2	2	2.379	1.7	1	0	3	2.404	5.0	5	1	1	2.464	11.0
4	2	0	2.366	9.1	4	2	0	2.381	4.6	0	2	2	2.463	3.5
1	2	2	2.347	32.7	1	2	2	2.379	8.7	1	2	2	2.427	16.7
6	0	1	2.264	5.3	4	1	2	2.368	1.7	4	2	0	2.403	5.2
2	2	2	2.258	2.8	2	2	2	2.285	7.1	2	0	3	2.365	1.9
0	1	3	2.255	2.1	4	2	1	2.264	20.9	0	1	3	2.340	2.2
4	2	1	2.249	19.6	6	0	1	2.252	2.6	2	2	2	2.327	4.8
6	1	0	2.230	1.1	5	0	2	2.243	10.0	1	1	3	2.309	3.2
1	1	3	2.228	4.6	6	1	0	2.220	1.1	4	2	1	2.289	20.7
2	1	3	2.151	7.8	2	1	3	2.171	6.4	5	0	2	2.269	1.3
3	2	2	2.129	7.3	3	0	3	2.168	1.1	6	0	1	2.261	4.7
5	1	2	2.115	3.0	3	2	2	2.150	1.6	6	1	0	2.228	1.3
3	1	3	2.039	10.5	6	1	1	2.125	1.6	2	1	3	2.223	4.9
5	2	1	2.034	6.9	3	1	3	2.054	7.7	3	0	3	2.216	1.0
2	3	0	2.018	7.1	2	3	0	2.049	10.3	3	2	2	2.186	4.6
4	0	3	2.001	5.8	4	0	3	2.010	7.5	5	1	2	2.143	2.6

TABLE 7
Cell Parameters of $AV_2O(PO_4)_2$ (A = Cd, Ca, Sr) Polycrystalline Phases

Phase	a (Å)	b (Å)	c (Å)	V (Å^3)
$CdV_2O(PO_4)_2$	14.3018(6)	6.3117(2)	7.2437(2)	653.9(2)
$CaV_2O(PO_4)_2$	14.198(1)	6.4214(6)	7.3160(8)	667.0(2)
$SrV_2O(PO_4)_2$	14.2250(8)	6.5169(3)	7.5216(3)	696.3(1)

TABLE 8
Paramagnetic Parameters in $AV_2O(PO_4)_2$ Phases

Phases	C_M (emu/mol)	θ (K)	μ_{eff}/μ_B
$CdV_2O(PO_4)_2$	2.12	34.2	2.94
$CaV_2O(PO_4)_2$	1.875	43.4	2.76
$SrV_2O(PO_4)_2$	1.625	44.4	2.58

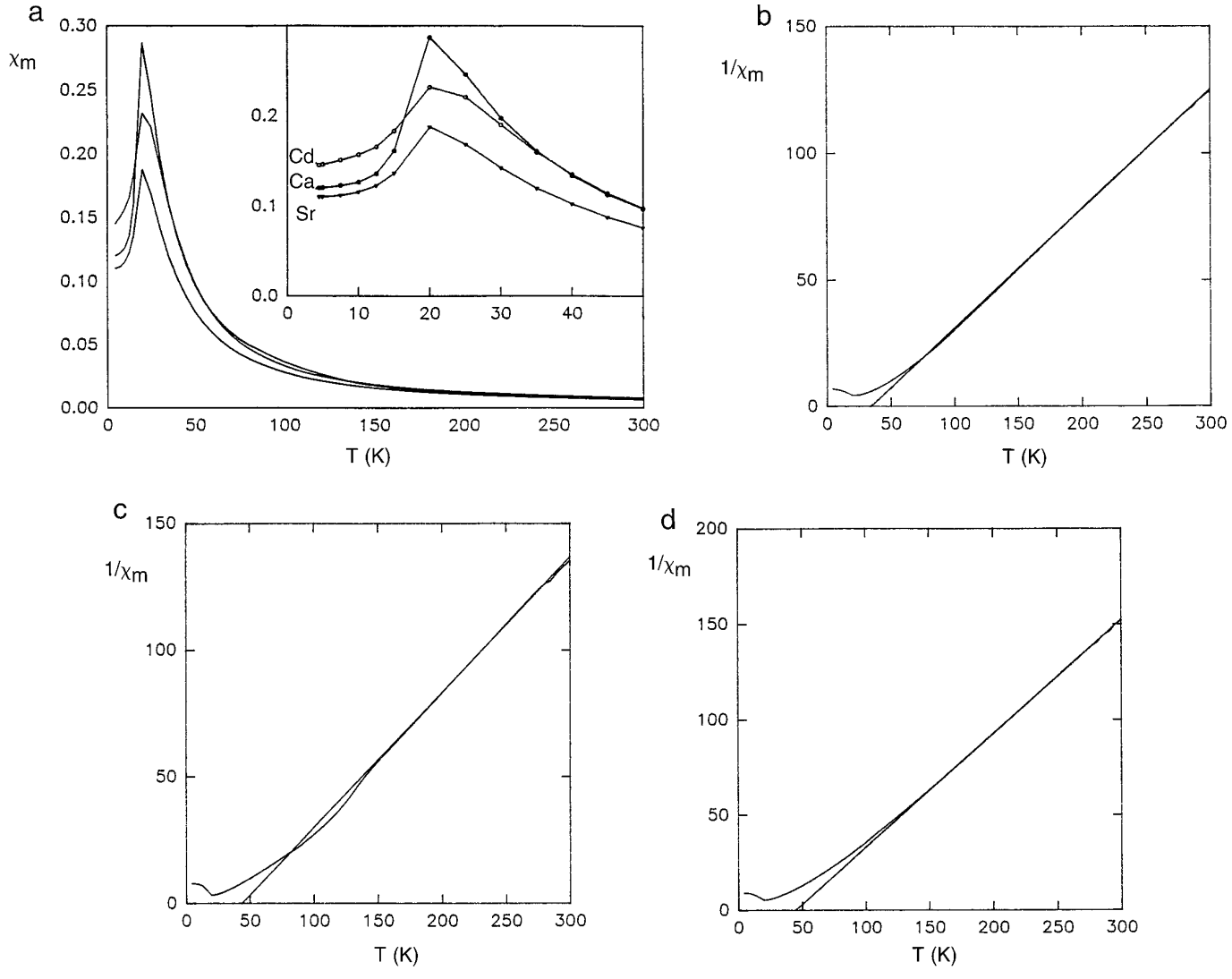

FIG. 2. (a) χ_M vs T for $AV_2O(PO_4)_2$ phases; (b) $1/\chi_M$ vs T for the Cd phase; (c) $1/\chi_M$ vs T for the Ca phase; (d) $1/\chi_M$ vs T for the Sr phase.

The magnetic behavior of these phases is significantly different from that of the VPO_4 compound that is also built up from similar $[VO_2]_\infty$ rutile chains. The $\chi_M(T)$ curve of the latter vanadium (III) phosphate also exhibits an antiferromagnetic transition, but in that case the transition is broad and spreads over 100 K, revealing a one-dimensionnal magnetic behavior. The V(2)–V(2) distances in these phosphates (3.159(1) to 3.257(1) Å) close to those observed in VPO_4 (3.142(1) Å) cannot explain this difference. In fact, for the monophosphates $AV_2O(PO_4)_2$, the antiferromagnetic spins coupling within the V(2) rutile chains may be significantly weakened by the proximity of the V(1) octahedra (Fig. 1), which creates a competitive V(2)–V(1)–V(2) triangular spin configuration; it results in a narrow transition, spreading over 20 K, with probably noncolinear vector spins.

A neutron diffraction study, and an appropriate crystal growth of these phases in view of studying their transport properties, will be necessary to understand the relationships between their physical properties and their low dimensional character.

REFERENCES

1. S. Boudin, A. Grandin, A. Leclaire, M. M. Borel, and B. Raveau, *J. Solid State Chem.* **111,** 380 (1994).
2. S. Boudin, A. Grandin, A. Leclaire, M. M. Borel, and B. Raveau, *Acta Crystallogr. Sect. C* **51,** 796 (1995).
3. N. Kinomura, F. Muto, and M. Koizumi, *J. Solid State Chem.* **45,** 252 (1982).
4. J. R. Carvajal, Fullprof 2.6.1, LLB, Sarclay, France, 1994.
5. S. R. Hall, H. D. Flack, and J. M. Stewart, Xtal 3.2 program, University of Western Austrialia, 1992.